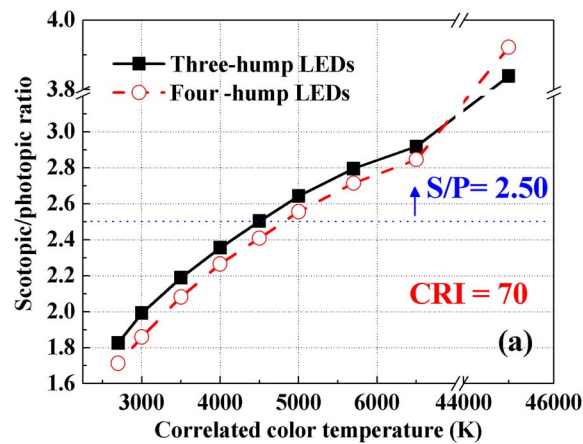


Studies of Scotopic/Photopic Ratios for Color-Tunable White Light-Emitting Diodes

Volume 5, Number 4, August 2013

Zi-Quan Guo
Tien-Mo Shih
Yi-Jun Lu
Yu-Lin Gao
Li-Hong Zhu
Guo-Long Chen
Ji-Hong Zhang
Si-Qi Lin
Zhong Chen



DOI: 10.1109/JPHOT.2013.2273736
1943-0655/\$31.00 ©2013 IEEE

Studies of Scotopic/Photopic Ratios for Color-Tunable White Light-Emitting Diodes

Zi-Quan Guo,¹ Tien-Mo Shih,^{1,2} Yi-Jun Lu,¹ Yu-Lin Gao,¹ Li-Hong Zhu,¹
Guo-Long Chen,¹ Ji-Hong Zhang,¹ Si-Qi Lin,¹ and Zhong Chen¹

¹Department of Electronic Science, Fujian Engineering Research Center for Solid-State Lighting,
State Key Laboratory of Physical Chemistry of Solid Surfaces,
Xiamen University, Xiamen 361005, China

²OAEE, College of Engineering, The University of Maryland, College Park, MD 20742 USA

DOI: 10.1109/JPHOT.2013.2273736
1943-0655/\$31.00 ©2013 IEEE

Manuscript received June 20, 2013; revised July 12, 2013; accepted July 12, 2013. Date of publication July 17, 2013; date of current version July 26, 2013. This work was supported in part by the Major Science and Technology Project between University–Industry Cooperation in Fujian Province under Grant 2011H6025, by the NNSF of China under Grant 11104230, and by the Key Project of Fujian Province under Grant 2012H0039. Corresponding authors: T. M. Shih and Z. Chen (e-mail: tmshih@xmu.edu.cn; chenz@xmu.edu.cn).

Abstract: Three- and four-hump InGaN-based white light-emitting diodes (LEDs) have been computationally investigated. The investigation includes three-hump LEDs precoated with green- and red-emitting quantum dots (QDs) and four-hump LEDs precoated with green-, yellow-, and red-emitting QDs. Results show scotopic/photopic (S/P) ratios > 3.80 and color rendering indices (CRIs) ≥ 70 for three-hump LEDs and S/P ratios > 3.90 and CRIs ≥ 70 for four-hump LEDs under a correlated color temperature (CCT) of 45 000 K. Furthermore, for both three- and four-hump LEDs under the condition of CCT > 5000 K, optimal results in this paper exhibit capabilities of exceeding S/P = 2.50 and simultaneously satisfying the criterion of CRI ≥ 70 . Our simulation procedure is conducted under variations of nine CCTs, several wavelengths, and peak heights. Optimized results of S/P ratios and CRIs are identified and retained through filtering off a great number of unqualified candidates. Finally, present findings may help improve the quality of eye visions pertaining to LED illumination and help reduce the electrical energy consumption related to LED usage.

Index Terms: Solid-state lighting, light-emitting diodes, scotopic/photopic ratios, color rendering index, luminous efficacy of radiation.

1. Introduction

For approximately a couple of decades, GaN-based white light-emitting diodes (LEDs) pre-coated with traditional phosphors (such as YAG : Ce³⁺) have been developed and have become widely used, partly due to their compact sizes, life longevity, low energy consumption, and especially high luminous efficacies (LE) [1]–[3]. Recent advances in such white LEDs have been driven primarily by the availability and progresses in III-Nitride LEDs resulting in significantly improved device technology. Various approaches have been pursued to address charge separation issues in InGaN-based quantum wells [4]–[8], material epitaxy optimization by using nano-patterned sapphire [9]–[11], efficiency droop [12]–[16], and light extraction [17]–[19] in III-Nitride LEDs. Some of these LEDs show the characteristic of LE > 250 lm/W [20]. However, there exists another criterion, known as scotopic/photopic (S/P) ratio that is intimately related to eye visions and energy savings [21], [22], and is defined as the ratio of a/b (a: luminous flux of a light source according to the Commission Internationale de l’Éclairage (CIE) scotopic spectral luminous efficiency function; b: luminous flux of a

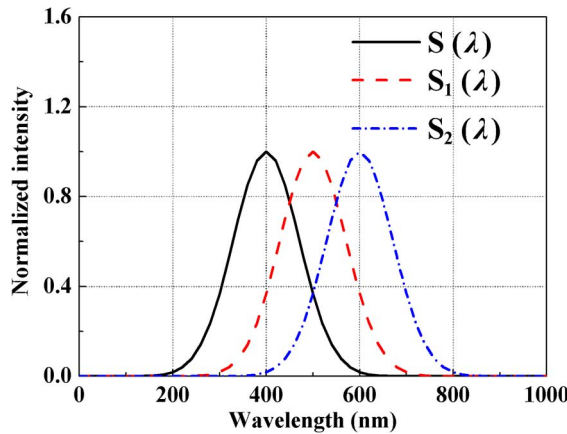


Fig. 1. Three Gaussian humps used to qualitatively explain magnitudes of integrals containing multiplications of two hump functions.

light source according to the CIE photopic spectral luminous efficiency function) [21]–[23]. Under the same luminous levels, the higher the S/P ratios become, the more the eye pupils shrink [21], [22]. This criterion is generally low ($S/P < 2.50$) for many of these LEDs, thus prompting researchers to seek other materials for substitution. Recently, quantum dots (QDs) have attracted considerable attention due to their favorable properties, including tunable emission wavelengths, narrow bandwidths, and reasonable quantum efficiencies [3], [22]. Because of the pre-coating, associated S/P ratios are elevated to higher than 2.50, and have been reported. In 2010, high S/P white LEDs fabricated from CdSe-silica QDs were experimentally investigated [24]. These phosphor materials, which were made from 5.5 nm nano-particles, have been found to exhibit an S/P ratio of 2.56 and color rendering index (CRI) of 86.63 at a correlated color temperature (CCT) of 5368 K. In 2011, Nizamoglu experimentally demonstrated high S/P single-chip white LEDs integrated with CdSe/ZnS core/shell QDs (with a high S/P ratio of 3.05 at a CCT of 45 000 K) [25]. These reported results are primarily experimental work, which can generally be guided and enhanced by computational simulations. Here, we investigate S/P ratios for three-hump and four-hump color-tunable white LEDs. Nine CCTs (2700 K, 3000 K, 3500 K, 4000 K, 4500 K, 5000 K, 5700 K, 6500 K, and 45 000 K) are considered, with some interesting findings to be discussed.

2. Experiments

In this paper, following parameters are considered: color rendering index (CRI) [26], color quality scale (CQS) [27], luminous efficacy of radiation (LER) [28], correlated color temperature (CCT) [29], and scotopic/photopic (S/P) ratio. Among them, the S/P ratio is emphasized, with its definition as [21]–[23]

$$S/P = \frac{K'}{K} = \frac{1700 \times \int_{380}^{780} S(\lambda) V'(\lambda) d\lambda}{683 \times \int_{380}^{780} S(\lambda) V(\lambda) d\lambda} \quad (1)$$

where K' denotes the luminous flux of a light source according to the CIE scotopic spectral luminous efficiency function; K stands for the luminous flux related to the CIE photopic spectral luminous efficiency function; $S(\lambda)$ is the spectral power distribution (SPD) of a light source; $V(\lambda)$ is the normalized CIE photopic spectral luminous efficiency function; $V'(\lambda)$ is the normalized CIE scotopic spectral luminous efficiency function. For human light-adaptive vision, cone photoreceptors play a dominant role, and their sensitivity peaks at 555 nm [22]. On the other hand, for human dark-adaptive vision, rod photoreceptors' sensitivity peaks at 507 nm. Incidentally, it is somewhat interesting to learn that the value of the integral containing two overlapped humps is normally greater than that containing two further-separated humps. For example, as shown in Fig. 1,

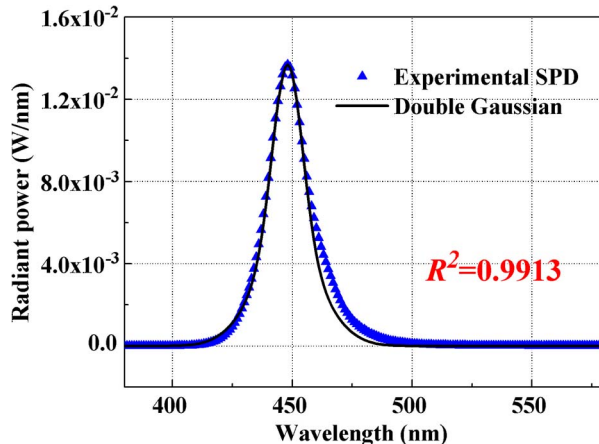


Fig. 2. Experimental SPDs versus the double Gaussian function.

$\int_0^{1000} S(\lambda) S_1(\lambda) d\lambda = 76$ is numerically found to be greater than $\int_0^{1000} S(\lambda) S_2(\lambda) d\lambda = 17$. This information can help enhance the clarity when we discuss later the trend of S/P, evaluated by Eq. (1), as a function of CCT.

Next, let us use the double Gaussian model for simulations of narrow-band SPDs of chips or QDs [30], [31]. It can be written as

$$\begin{aligned} S(\lambda) &= H_p \times [G(\lambda) + 2 \times G^5(\lambda)]/3 \\ G(\lambda) &= \exp\left[-(\lambda - \lambda_p)^2/w_b^2\right] \end{aligned} \quad (2)$$

where H_p , λ_p , and w_b represent the peak height, peak wavelength, and bandwidth (or known as full-width at half-maxima, FWHM). It is beneficial to compare the shape of this theoretical hump with experimental measurements.

Experimental SPDs were obtained by measuring the spectra of InGaN-based multiple-quantum-well (MQW) blue LEDs, which were fabricated by using the metal organic chemical vapor deposition (MOCVD), with an area of 1 mm². During measurements, samples were placed on the temperature-controlled heat sink, which was maintained at 300 K by Keithley 2510. The meter of Keithley 2611 was used to supply a current of 350 mA for illumination of LEDs. Finally, spectra were measured by using the SP320 spectrometer with an integration sphere manufactured by Instrument Systems Inc.

In Fig. 2, experimental SPD of blue chips and the double Gaussian function are plotted versus the wavelength for $R^2 > 0.99$. A close agreement of these two curves is observed, and such closeness suggests that the analytical function shown in the figure can be safely used for filtering simulations. Since the SPDs of QDs also exhibit the Gaussian shape [24], [25], [31], the same model can be used for all humps.

Hence, the SPDs of three-hump and four-hump white LEDs can be given, respectively, as

$$\begin{aligned} S_{\text{three-hump}}(\lambda) &= S_B(\lambda) + S_G(\lambda) + S_R(\lambda) \\ S_{\text{four-hump}}(\lambda) &= S_B(\lambda) + S_G(\lambda) + S_Y(\lambda) + S_R(\lambda). \end{aligned} \quad (3)$$

Ranges of wavelength are: (1) 430 ~ 490 nm (blue, B), 500 ~ 590 nm (green, G), and 600 ~ 660 nm (red, R) for three-hump white LEDs; (2) 430 ~ 490 nm (blue, B), 500 ~ 540 nm (green, G), 550 ~ 590 nm (yellow, Y), and 600 ~ 660 nm (red, R) for four-hump white LEDs. Bandwidths of all narrow bands are 30 nm for convenience. These characteristic parameters are listed in Tables 1 and 2 given in the Appendix.

In general, there exists a tradeoff between CRI and S/P. Since the objective of this study is in search of maximum S/P ratios, an optimization procedure is needed. The filtering procedure of such optimization can be found in the literature in detail [31]. The filtering conditions in this work are

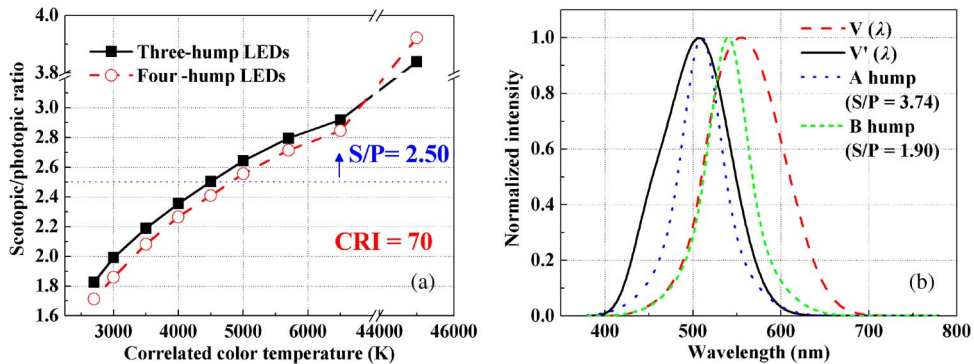


Fig. 3. (a) S/P ratios versus CCTs for three-hump white LEDs and four-hump white LEDs, and (b) shifts of hump B towards hump A.

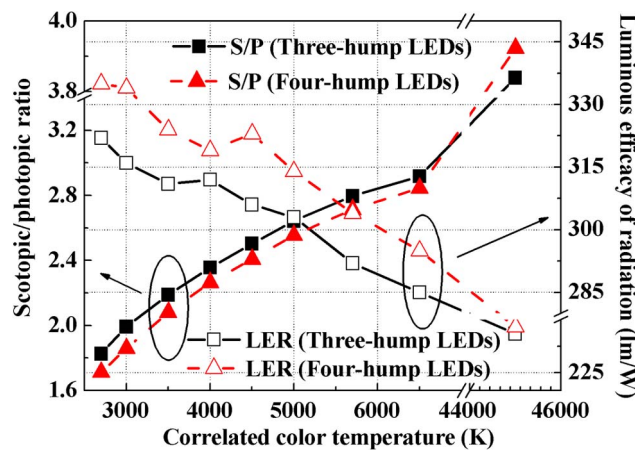


Fig. 4. S/P ratios and LERs versus CCTs for three-hump white LEDs and four-hump white LEDs.

specified as: $CRI \geq 70$, $CQS \geq 60$, and color distance (D_{uv}) < 0.0054 [26]. They are so selected because (1) the value of 70 can satisfy basic CRI performances, and (2) comparisons with experimental results in [25] can be conducted. For CCT specifications, we wish to vary as minimally as possible. To achieve this goal, we take increments of 10 K surrounding eight frequently-used values (namely, 2700 K, 3000 K, 3500 K, 4000 K, 4500 K, 5000 K, 5700 K, and 6500 K), and an increment of 1000 K surrounding 45 000 K.

3. Results and Discussion

Fig. 3(a) shows the S/P ratios versus CCTs. It is observed that the ratio increases as CCT increases. The S/P ratio is larger than 3.80 for three-hump white LEDs and 3.90 for four-hump white LEDs, respectively, at CCT = 45 000 K. Overall, these values are slightly higher than experimental counterparts [25]. In general, conditions for $S/P > 2.50$ and $CCT > 5000$ K are recommended. For example, at CCT = 2700 ~ 3000 K, the incandescent light bulbs exhibit 1.41 [25], which is lower than 1.70 observed from the Figure. With the introduction of Fig. 1, now we understand more readily why S/P increases as CCT increases. It is known that both S/P ratios and CCT values are generally proportional to percentages of shorter wavelengths in the visible light range. Fig. 3(b) indicates that CCT increases (or S/P increases from 1.90 increases to 3.74) as hump B shifts toward hump A.

In Fig. 4, S/P ratio and LER are plotted versus CCT to show the contrast for both three-hump and four-hump white LEDs. Since LER is expressed in the denominator in Eq. (1), it is expected to exhibit the opposite trend to S/P ratios. If optimizing both criteria of S/P ratios and LER values is

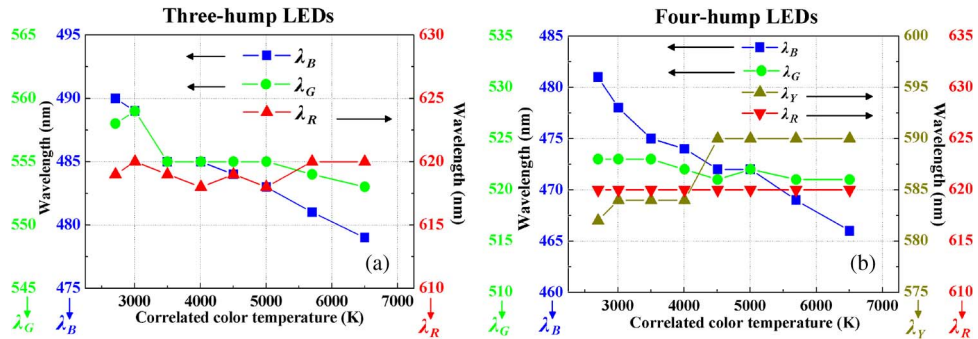


Fig. 5. Optimal peak wavelengths versus CCTs for (a) three-hump white LEDs and (b) four-hump white LEDs.

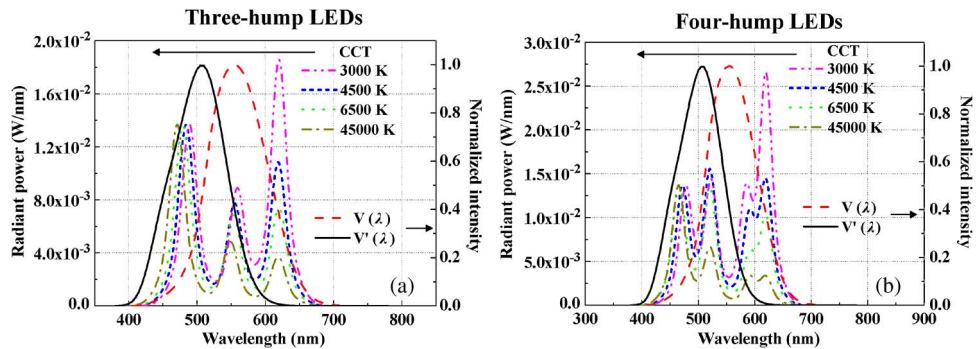


Fig. 6. Optimal SPDs and scotopic and photopic sensitivity functions versus wavelengths for (a) three-hump white LEDs and (b) four-hump white LEDs.

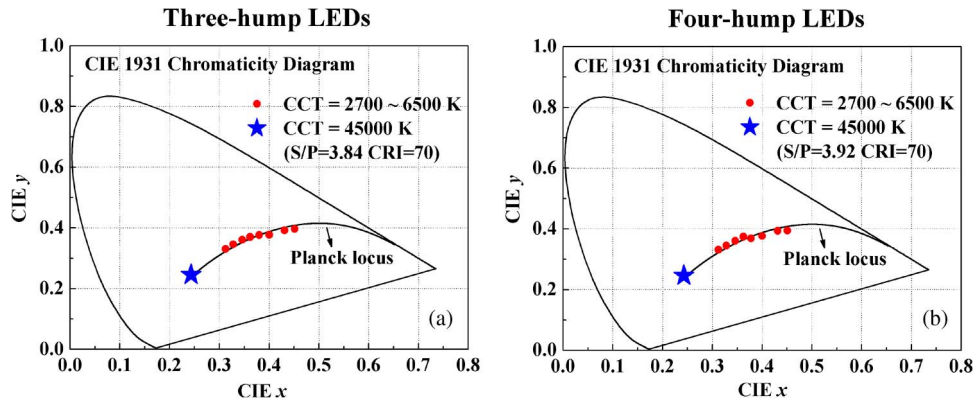


Fig. 7. Color coordinates of optimal SPDs in the CIE 1931 diagram for (a) three-hump white LEDs and (b) four-hump white LEDs.

desired, we can select the intersection of two curves for three-hump white LEDs and the same for four-hump white LEDs.

The wavelength versus CCT for both three-hump and four-hump LEDs is plotted in Fig. 5. In Fig. 5(a), relatively drastic variations are observed for the blue hump, suggesting that, under different CCT values, large numerical variations should be taken during simulations. Between 3000 K and 3500 K of CCT values, the green wavelength drastically decreases, and remains unchanged

TABLE 1

Ranges and increments of parametric values for three-hump white LEDs

Color	Wavelength (nm) ($\Delta\lambda = 1$)	FWHM (nm) ($\Delta\omega = 1$)	Peak height (mW) ($\Delta H = 0.01$)
Blue	430-490	30-30	13.69-13.69
Green	500-590	30-30	1.00-30.00
Red	600-660	30-30	1.00-30.00

TABLE 2

Ranges and increments of parametric values for four-hump white LEDs

Color	Wavelength (nm) ($\Delta\lambda = 1$)	FWHM (nm) ($\Delta\omega = 1$)	Peak height (mW) ($\Delta H = 0.01$)
Blue	430-490	30-30	13.69-13.69
Green	500-540	30-30	1.00-30.00
Yellow	550-590	30-30	1.00-30.00
Red	600-660	30-30	1.00-30.00

TABLE 3

Values of integrals expressed in the S/P ratios at CCT = 6500 K and 45 000 K for three-hump LEDs

CCT (K)	$\int_{380}^{780} S(\lambda) V'(\lambda) d\lambda$	$\int_{380}^{780} S(\lambda) V(\lambda) d\lambda$
6500	0.489	0.417
45000	0.533	0.346

elsewhere. For the red hump, wavelength ($\lambda_R = 620$ nm) variations are negligible, recommending us to keep same values. In Fig. 5(b), the trend of the blue hump for the four-hump case is similar to that of the three-hump case. Wavelengths for green and red humps remain leveled, while the yellow wavelength increases in the neighborhood of 4000 K and 4500 K CCT values.

Fig. 6 shows the radiant power versus the wavelength under four CCT values (3000 K, 4500 K, 6500 K, and 45 000 K). For clarity, the normalized photopic and scotopic spectral luminous efficiency functions are also included. This figure can be used to explain the trend shown in Fig. 3(a). For example, let us compare two cases at CCT = 6500 K and CCT = 45 000 K for three-hump white LEDs. In reference to Table 3, we can see that, at CCT = 6500 K, S/P value is equal to $a_1 * (0.489/0.417)$, and at CCT = 45 000 K, S/P value is equal to $a_1 * (0.533/0.346)$. Therefore, clearly the S/P value at CCT = 45 000 K is higher than that at CCT = 6500 K, because $0.533 > 0.489$ shown in the numerator and $0.346 < 0.417$ shown in the denominator. Note that $a_1 = 1700/683$.

In Fig. 7, color coordinates of optimal SPDs under nine CCTs for three-hump and four-hump white LEDs are plotted in the CIE 1931 diagram, with the blue star representing 45 000 K. It is noticed that these color coordinates nearly coincide with the Planck locus, indicating a close chromatic agreement between the simulated results and the black body under the same CCT. In comparison of Fig. 7(a) and (b), color coordinates are located more closely to Planck locus in the former.

In the Appendix, Table 4 shows some optimal results according to S/P ratios for three-hump white LEDs obtained in this optimization procedure. From Table 4, the maxima S/P is noticed to be 3.84 at CCT = 45 000 K along with the value of LER of 236 lm/W. The optimal wavelength of blue, yellow,

TABLE 4

The peak wavelengths, peak heights, photometric and colorimetric performances with CRI ≥ 70 and CQS ≥ 60 , and $D_{uv} < 0.0054$ at CCTs of 2700 K to 45 000 K for three-hump white LEDs

Target CCT (K)	2700	3000	3500	4000	4500	5000	5700	6500	45000
CCT (K)	2708	3006	3499	4009	4504	5005	5701	6502	44963
D_{uv}	0.0047	0.0039	0.0050	0.0003	0.0028	0.0044	0.0045	0.0043	0.0038
λ_B (nm)	490	489	485	485	484	483	481	479	471
λ_Y (nm)	558	559	555	555	555	555	554	553	549
λ_R (nm)	619	620	619	618	619	618	620	620	619
H_B (mW)	13.69	13.69	13.69	13.69	13.69	13.69	13.69	13.69	13.69
H_G (mW)	9.29	8.80	8.39	7.92	7.70	7.25	7.05	6.84	4.85
H_R (mW)	22.49	18.57	15.45	12.61	10.84	9.26	8.29	7.39	3.71
CRI	70	70	70	70	70	70	70	70	70
CQS	67	69	73	70	66	63	64	65	63
LER (lm/W)	322	316	311	312	306	303	292	285	236
S/P	1.83	1.99	2.19	2.36	2.50	2.64	2.80	2.92	3.84

TABLE 5

The peak wavelengths, peak heights, photometric and colorimetric performances with CRI ≥ 70 and CQS ≥ 60 , and $D_{uv} < 0.0054$ at CCTs of 2700 K to 45 000 K for four-hump white LEDs

Target CCT (K)	2700	3000	3500	4000	4500	5000	5700	6500	45000
CCT (K)	2701	3009	3502	4009	4509	5005	5695	6505	45597
D_{uv}	0.0054	0.0034	0.0051	0.0030	0.0046	0.0043	0.0039	0.0047	0.0040
λ_B (nm)	481	478	475	474	472	472	469	466	465
λ_G (nm)	523	523	523	522	521	522	521	521	521
λ_Y (nm)	582	584	584	584	590	590	590	590	591
λ_R (nm)	620	620	620	620	620	620	620	620	620
H_B (mW)	13.69	13.69	13.69	13.69	13.69	13.69	13.69	13.69	13.69
H_G (mW)	11.27	14.45	12.55	11.92	15.64	13.06	13.12	13.41	6.55
H_Y (mW)	13.69	12.17	9.69	8.83	9.39	7.78	6.56	5.03	2.98
H_R (mW)	28.18	26.61	19.39	15.45	13.69	10.89	9.98	9.78	2.98
CRI	70	70	70	70	70	70	70	70	70
CQS	67	73	74	76	67	69	69	69	67
LER (lm/W)	335	334	324	319	323	314	304	295	238
S/P	1.71	1.86	2.08	2.27	2.41	2.56	2.72	2.85	3.92

and red colors of these color-tunable white LEDs are located within 471 ~ 490 nm, 549 ~ 558 nm, and ~620 nm, respectively. Table 5 shows some simulation results for four-hump white LEDs. It is noticed that the S/P = 3.92 and LER = 238 lm/W at CCT = 45 000 K. The value of S/P ratio is a little higher than that for three-hump white LEDs. Optimal wavelengths of blue, green, yellow, and red colors of four-hump color-tunable white LEDs are located within 465 ~ 481 nm, ~ 522 nm, 582 ~ 591 nm, and ~620 nm, respectively.

4. Conclusion

We investigate three-hump and four-hump InGaN-based white light-emitting diodes (LEDs) by conducting simulations and optimizations. Results of scotopic/photopic (S/P) ratios > 3.80 and color rendering indices (CRI) ≥ 70 for three-hump LEDs as well as S/P > 3.90 and CRI ≥ 70 for four-hump LEDs under a CCT of 45 000 K have been obtained. Other results under 8 CCTs of 2700 K, 3000 K, 3500 K, 4000 K, 4500 K, 5000 K, 5700 K, and 6500 K have also been presented. Our finding confirms that S/P ratios increase as CCT values increase. Hopefully, the present study can serve as a reference for future experimental studies for multiple-hump LEDs.

Appendix

See Tables 1–5.

References

- [1] E. F. Schubert and J. K. Kim, "Solid-state light sources getting smart," *Science*, vol. 308, no. 5726, pp. 1274–1278, May 2005.
- [2] J. M. Phillips, M. F. Coltrin, M. H. Crawford, A. J. Fischer, M. R. Krames, R. Mueller-Mach, G. O. Mueller, Y. Ohno, L. E. S. Rohwer, J. A. Simmons, and J. Y. Tsao, "Research challenges to ultra-efficient inorganic solid-state lighting," *Laser Photon. Rev.*, vol. 1, no. 4, pp. 307–333, Dec. 2007.
- [3] H. V. Demir, S. Nizamoglu, T. Erdem, E. Mutlugun, N. Gaponik, and A. Eychmüller, "Quantum dot integrated LEDs using photonic and excitonic color conversion," *Nano Today*, vol. 6, no. 6, pp. 632–647, Dec. 2011.
- [4] R. M. Farrell, E. C. Young, F. Wu, S. P. DenBaars, and J. S. Speck, "Materials and growth issues for high-performance nonpolar and semipolar light-emitting devices," *Semicond. Sci. Technol.*, vol. 27, no. 2, pp. 024001-1–024001-14, Feb. 2012.
- [5] D. F. Feezell, J. S. Speck, S. P. DenBaars, and S. Nakamura, "Semipolar (20̄21̄) InGaN/GaN light-emitting diodes for high-efficiency solid-state lighting," *J. Display Technol.*, vol. 9, no. 4, pp. 190–198, Apr. 2013.
- [6] H. Zhao, G. Liu, J. Zhang, J. D. Poplawsky, V. Dierolf, and N. Tansu, "Approaches for high internal quantum efficiency green InGaN light-emitting diodes with large overlap quantum wells," *Opt. Exp.*, vol. 19, no. S4, pp. A991–A1007, Jul. 2011.
- [7] H. P. Zhao, G. Y. Liu, X. H. Li, R. A. Arif, G. S. Huang, J. D. Poplawsky, S. T. Penn, V. Dierolf, and N. Tansu, "Design and characteristics of staggered InGaN quantum-well light-emitting diodes in the green spectral regime," *IET Optoelectron.*, vol. 3, no. 6, pp. 283–295, Dec. 2009.
- [8] J. Zhang and N. Tansu, "Optical gain and laser characteristics of InGaN quantum wells on ternary InGaN substrates," *IEEE Photon. J.*, vol. 5, no. 2, p. 2 600 111, Apr. 2013.
- [9] Y.-K. Ee, J. M. Biser, W. Cao, H. M. Chan, R. P. Vinci, and N. Tansu, "Metal organic vapor phase epitaxy of III-nitride light-emitting diodes on nano-patterned AGOG sapphire substrate by abbreviated growth mode," *J. Sel. Topics Quantum Electron.*, vol. 15, no. 4, pp. 1066–1072, Jul./Aug. 2009.
- [10] Y.-K. Ee, X.-H. Li, J. Biser, W. Cao, H. M. Chan, R. P. Vinci, and N. Tansu, "Abbreviated MOVPE nucleation of III-nitride light-emitting diodes on nano-patterned sapphire," *J. Cryst. Growth*, vol. 312, no. 8, pp. 1311–1315, Apr. 2010.
- [11] Y. F. Li, S. You, M. W. Zhu, L. Zhao, W. T. Hou, T. Detchprohm, Y. Taniguchi, N. Tamura, S. Tanaka, and C. Wetzel, "Defect-reduced green GaInN/GaN light-emitting diode on nanopatterned sapphire," *Appl. Phys. Lett.*, vol. 98, no. 15, pp. 151102-1–151102-3, Apr. 2011.
- [12] S. Choi, M. H. Ji, J. Kim, H. J. Kim, M. M. Satter, P. D. Yoder, J. H. Ryou, R. D. Dupuis, A. M. Fischer, and F. A. Ponce, "Efficiency droop due to electron spill-over and limited hole injection in III-nitride visible light-emitting diodes employing lattice-matched InAlN electron blocking layers," *Appl. Phys. Lett.*, vol. 101, no. 16, pp. 161110-1–161110-5, Oct. 2012.
- [13] H. P. Zhao, G. Y. Liu, J. Zhang, R. A. Arif, and N. Tansu, "Analysis of internal quantum efficiency and current injection efficiency in III-Nitride light-emitting diodes," *J. Display Technol.*, vol. 9, no. 4, pp. 212–225, Apr. 2013.
- [14] G. Y. Liu, J. Zhang, C. K. Tan, and N. Tansu, "Efficiency-droop suppression by using large-bandgap AlGaN thin barrier layers in InGaN quantum wells light-emitting diodes," *IEEE Photon. J.*, vol. 5, no. 2, p. 2201011, Apr. 2013.
- [15] M. F. Schubert, J. Xu, J. K. Kim, E. F. Schubert, M. H. Kim, S. Yoon, M. Lee, C. Sone, T. Sakong, and Y. Park, "Polarization-matched GaInN/AlGaN multi-quantum-well light-emitting diodes with reduced efficiency droop," *Appl. Phys. Lett.*, vol. 93, no. 4, pp. 041102-1–041102-3, Jul. 2008.
- [16] C. K. Tan, J. Zhang, X. H. Li, G. Y. Liu, B. O. Tayo, and N. Tansu, "First-principle electronic properties of dilute-As GaNAs alloy for visible light emitters," *J. Display Technol.*, vol. 9, no. 4, pp. 272–279, Apr. 2013.
- [17] J. Jewell, D. Simeonov, S. C. Huang, Y. L. Hu, S. Nakamura, J. Speck, and C. Weisbuch, "Double embedded photonic crystals for extraction of guided light in light-emitting diodes," *Appl. Phys. Lett.*, vol. 100, no. 17, pp. 171105-1–171105-4, Apr. 2012.
- [18] P. F. Zhu, G. Y. Liu, J. Zhang, and N. Tansu, "FDTD analysis on extraction efficiency of GaN light-emitting diodes with microsphere arrays," *J. Display Technol.*, vol. 9, no. 5, pp. 317–323, May 2013.
- [19] X. H. Li, P. F. Zhu, G. Y. Liu, J. Zhang, R. B. Song, Y. K. Ee, P. Kumnorkaew, J. F. Gilchrist, and N. Tansu, "Light extraction efficiency enhancement of III-Nitride light-emitting diodes by using 2-D close-packed TiO₂ microsphere arrays," *J. Display Technol.*, vol. 9, no. 5, pp. 324–332, May 2013.

- [20] [Online]. Available: <http://www.cree.com/news-and-events/cree-news/press-releases/2012/april/120412-254-lumen-per-watt>
- [21] S. M. Berman, "Energy efficiency consequences of scotopic sensitivity," *J. Illumin. Eng. Soc.*, vol. 21, no. 1, pp. 3–14, Winter 1992.
- [22] T. Erdem and H. V. Demir, "Color science of nanocrystal quantum dots for lighting and displays," *Nanophotonics*, vol. 2, no. 1, pp. 57–81, Mar. 2013.
- [23] Commission Internationale de l'Éclairage (CIE), Recommended system for mesopic photometry based on visual performance, Central Bureau CIE, Vienna, Austria, Tech. Rep. 191:2010, 2010.
- [24] A. Lita, A. L. Washington, L. van de Burgt, G. F. Strouse, and A. E. Stiegman, "Stable efficient solid-state white-light-emitting phosphor with a high scotopic/photopic ratio fabricated from fused CdSe–silica nanocomposites," *Adv. Mater.*, vol. 22, no. 36, pp. 3987–3991, Sep. 2010.
- [25] S. Nizamoglu, T. Erdem, and H. V. Demir, "High scotopic/photopic ratio white-light-emitting diodes integrated with semiconductor nanophosphors of colloidal quantum dots," *Opt. Lett.*, vol. 36, no. 10, pp. 1893–1895, May 2011.
- [26] Commission Internationale de l'Éclairage (CIE), Method of specifying and measuring color rendering properties of light sources, Central Bureau CIE, Vienna, Austria, CIE Publ. 13.3, 1995.
- [27] W. Davis and Y. Ohno, "Color quality scale," *Opt. Eng.*, vol. 49, no. 3, pp. 033602-1–033602-16, Mar. 2010.
- [28] A. Ukauskas, R. Vaicekauskas, F. Ivanauskas, R. Gaska, and M. S. Shur, "Optimization of white polychromatic semiconductor lamps," *Appl. Phys. Lett.*, vol. 80, no. 2, pp. 234–236, Jan. 2002.
- [29] A. R. Robertson, "Computation of correlated color temperature and distribution temperature," *J. Opt. Soc. Amer.*, vol. 58, no. 11, pp. 1528–1535, Nov. 1968.
- [30] Y. Ohno, "Spectral design considerations for white LED color rendering," *Opt. Eng.*, vol. 44, no. 11, pp. 111302-1–111302-9, Nov. 2005.
- [31] Z. Q. Guo, T. M. Shih, Y. L. Gao, Y. J. Lu, L. H. Zhu, G. L. Chen, Y. Lin, J. H. Zhang, and Z. Chen, "Optimization studies of two-phosphor-coated white light-emitting diodes," *IEEE Photon. J.*, vol. 5, no. 2, p. 8200112, Apr. 2013.